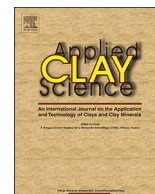




Contents lists available at ScienceDirect

Applied Clay Science

journal homepage: www.elsevier.com/locate/clay

Research paper

Identifying the differences between clays used in the brick industry by various methods: Iron extraction and NMR spectroscopy

Julie Peyne^{a,b}, Ameni Gharzouni^a, Isabel Sobrados^c, Sylvie Rossignol^{a,*}^a Univ. Limoges, IRCER, UMR 7315, F-87000 Limoges, France^b Bouyer Leroux, L'établère 44210, La Séguinière, France^c Instituto de Ciencia de Materiales de Madrid, Consejo Superior de Investigaciones Científicas (CSIC), C/Sor Juana Inés de la Cruz, 3, 28049 Madrid, Spain

ARTICLE INFO

Keywords:

Clay minerals
Iron
NMR spectroscopy
Calcination
Bricks clay

ABSTRACT

This study focused on identifying the differences in a clay quarry that is used in brick production to understand the variation between samples based on two kinds of clays: the first kind was suitable for brick production, but the second one did not show good production efficiency. Various samples were characterized by physical and chemical methods. In addition, free iron extraction by a CBD method and calcination at various temperatures were performed. The clay samples were then structurally characterized by XRD, FTIR and ²⁷Al NMR spectroscopy and thermally characterized using dilatometry. Finally, these results were correlated to the SEM investigation. These results revealed variations in the Si/Al molar ratio (1.4 to 3.3) due to the mineralogy variation within the quarry. Indeed, the non-secondary phase and clay phase contents differed according to the location in the quarry. NMR analysis also revealed that some iron atoms were located in a kaolinite structure, whereas other iron phases, in goethite form, interacted with clay minerals only on the surface of, e.g., kaolinite and muscovite and were not in their structures. From the thermal characterization, the influence of this structural iron in the kaolinite was also evidenced by an increase in the total shrinkage. In conclusion, this work determined the structural differences and their impact on brick production.

1. Introduction

Clay minerals are characterized by several physical and chemical properties, such as their swelling behavior, cation exchange capacity (CEC), cation adsorption, and high surface area (Bergaya and Lagaly, 2013) that cause these raw materials to be used strategically in numerous industrial applications, such as brick production (Gualtieri et al., 2015).

Conventionally, bricks are made from a mixture of numerous clays extracted from different quarries (Kornmann, 2009). The final properties of the bricks (e.g., presence of failures, color, durability, compressive strength) clearly depend on the raw materials used. Nonetheless, the non-homogeneous mineralogy content of the brick clay mixture creates difficulties in understanding the impact of each mineral from each quarry. However, it is well known that an increase in the montmorillonite content leads to technical issues during the drying step due to increases in the shrinkage and capillarity retention (Sigg, 1991). In addition, the final color of the brick is clearly due to the initial iron content (Li et al., 2016). The presence of kaolinite also increases the plasticity of the brick mixture, thereby improving the mixture

preparation (Jimenez-Quero et al., 2017). Even if it were possible to separately determine the contribution of each mineral to the properties of the mixture, the characterization techniques used in the industry (mainly the particle size distribution, chemical analysis and mineralogy) would not allow the suitability of the clay for brick production to be determined. The most advanced techniques, such as ²⁷Al NMR and SEM microscopy, are expensive and thus not yet in use. However, several previous reports demonstrated that ²⁷Al NMR spectroscopy is a very powerful tool for deeply investigating the crystal chemistry of layered silicates such as kaolinite, montmorillonite, and muscovite (Thompson, 1984; Woessner, 1989; Takahashi et al., 2008). For example, it is possible to evaluate the evolution of the 6-, 5- and 4-coordinate aluminum sites with temperature during the dehydroxylation reaction of kaolinite (Benharrats et al., 2003; Wanabe et al., 1987), thus revealing the conversion of the 6-coordinate into 5- and 4-coordinate aluminum. The structures of the clays considered for this application are not often described in the literature. However, Mackenzie et al. (1987) studied the thermal transformations of muscovite and used ²⁷Al and ²⁹Si NMR to demonstrate that iron impurities lead to an increase in recrystallization and favor the mullite to corundum conversion. In

* Corresponding author.

E-mail address: Sylvie.rossignol@unilim.fr (S. Rossignol).<https://doi.org/10.1016/j.clay.2018.02.037>Received 12 October 2017; Received in revised form 23 February 2018; Accepted 25 February 2018
0169-1317/ © 2018 Elsevier B.V. All rights reserved.

addition, Wei et al., 2012 highlighted the impact of goethite in a kaolinite-goethite mixture or in a goethite interaction with kaolinite, revealing a 6-coordinate aluminum contribution at a lower chemical shift for the goethite-kaolinite mixture than for the goethite interaction with kaolinite (3.04 and 5.76 ppm, respectively). It is also possible to detect the kaolinite defect in the structure and, more precisely, the iron in the kaolinite structure, as described by Schroeder and Pruett, 1996. ^{27}Al NMR is thus an appropriate structural characterization method for studying the impact of impurities on clay minerals. It is clear that the iron oxide and (hydr)oxide contents can influence the clay structure. Differences within a clay quarry could thus occur (Guzlena et al., 2017) and lead to technical issues after numerous steps of brick production. Thus, this study aims to understanding the differences in a clay quarry and their influence on the quality of brick production. To achieve this goal, two lots of clay with different impacts on brick production were extracted in northwest France. Chemical treatments, such as a free iron extraction and thermal treatment (with various calcinations at two temperatures: 350 and 700 °C), were then performed to demonstrate the influence of the iron and the thermal behavior of each clay. Next, the physical and chemical features and structural information were obtained by X-ray powder diffraction, FTIR and ^{27}Al NMR spectroscopy. These results were then correlated to the thermal behavior of the clays before and after the chemical and thermal treatments.

2. Experimental

2.1. Raw materials and samples preparation

Numerous samples (18) from one quarry that is located in northwest France and used in the brick industry were selected for this study. Two different lots of samples (A and B) with two distinct sets of visual characteristics, such as color and grain size, were observed. They were also selected according to their influence on brick production, i.e., on the scrap rate after the sintering of bricks. Indeed, A samples were suitable for brick production, but B samples were not suitable because they led to a significant increase in the scrap rates after the sintering step. The sampling was performed based on the height of the rock face.¹ The preparation of these samples was divided into two steps: (i) drying for 24 h at 40 °C and (ii) coarse grinding (< 1 mm). The red/yellow/brown color of these samples clearly demonstrates the presence of iron oxohydroxide (Cornell and Schwertmann, 2002). Using the Mehra and Jackson procedure (Mehra and Jackson, 1960), free iron oxide (organic complexes, amorphous and highly crystallized forms) can be totally dissolved. The main reactants used are a Na-citrate solution (0.3 M) and a NaHCO_3 solution (1 M), with sodium dithionite ($\text{Na}_2\text{S}_2\text{O}_4$). A suitable amount of the clay sample (4 g) was mixed with 40 mL of the Na citrate solution and 5 mL of 1 M NaHCO_3 in a water bath (80 °C). Then, 1 g of $\text{Na}_2\text{S}_2\text{O}_4$ was added, mixed continuously for 1 min and then mixed occasionally for 15 min. Then, 10 mL of a saturated NaCl solution was added and centrifuged for 5 min (at 2500 rpm/min). Finally, the supernatant was decanted into a flask, and the residual solid was kept and dried at 40 °C for 24 h. To characterize the temperature behavior, various calcinations in an electrical furnace for bulk samples before and after the iron extraction were performed at 350 and 700 °C (T), which corresponded to the temperatures after iron (hydr)oxide decomposition and clay minerals dihydroxylation, respectively (Ruan et al., 2002; Lopez et al., 2011). The following nomenclature is used: A/B_y-C-T, where y specifies the number of the sample, C is the performed chemical treatment and T is the calcination temperature.

2.2. Characterization techniques

The mineral phases of the samples (either calcined or not) were

identified by XRD with a BRUKER AXS D8 Advance powder diffractometer using $\text{CuK}\alpha$ radiation ($\lambda\alpha = 0.154186$ nm). The investigated 2theta range used was between 2.5 and 65°, with a step size of 0.012° (2theta) and an acquisition time of 2 s per step. JCPDS files (Joint Committee Powder Diffraction Standard) were used for the principal phase identification.

High-resolution MAS-NMR experiments were performed at room temperature using a Bruker AVANCE-400 spectrometer operating at 104.26 MHz (^{27}Al signal) on powder samples, which were spun at 10 KHz. The number of scans was 400 (Autef et al., 2013). In order to record the central transitions of aluminum (^{27}Al) ($I = 5/2$), a $\pi/8$ (1.5 μs) pulse was applied to it and 1 MHz filter was used. A recycle delay of 5 s was chosen to minimize saturation effects. Chemical shift values were given with reference to an external aqueous AlCl_3 solution. The relative areas of the components were determined using DMFIT program.

Diffuse reflectance spectra of the clay minerals (in powder form) were obtained between 300 and 780 nm with a CARY 500 spectrophotometer (cf. Supplementary files). A remission function (also called the Kubelka Munk function, Kubelka and Munk, 1931; Barron and Torrent, 1986) was applied to the experimental data according to the literature, with $f(R) = \frac{(1-R)^2}{2R}$, where R is the reflexion. Noise reduction was then performed by fitting each Kubelka Munk spectrum with an Adjacent Averaging (5 points) method. Finally, the second derivate was calculated using Origin V8.

Dilatometric measurements were made under air by means of a contact horizontal dilatometer (NETZSCH DIL 402C) on clay samples pressed with a cylindrical geometry (H = 10 mm; $\varnothing = 6.5$ mm). Two alumina (Al_2O_3) holders were placed at the surface end contacts of the samples to prevent high-temperature diffusion between the samples and the alumina rod. A calibration cycle (with a standard sample of Al_2O_3) was performed and registered. The calibration data were then subtracted from the data collected for each sample to eliminate the contribution from the device. The thermal cycle used consisted of heating at 10 °C/min to 1100 °C and cooling to 25 °C at a similar cooling rate.

3. Results and discussion

3.1. Physical and chemical characterization

The physical and chemical features of two sample sets (y = 1, 2, 3, 4) for the A_y-25 and B_y-25 lots are presented in Table 1. No significant variation is observed in the weight percentage of the > 40 μm granulometry range (31–45 and 36–46 wt% for B_y and A_y, respectively). Nonetheless, an increase in the total fraction of the 40–80 μm range can be observed for the B_y lot (8–15 and 5–6 wt% for A_y and B_y, respectively). The specific surface area (S_{BET}) and cation exchange capacity (CEC) values depend on the sampling lot, and they vary with the same behavior. Indeed, higher S_{BET} and CEC values are obtained for A_y than B_y (27 m²/g – 11.6 cmol₍₊₎/kg and 17 m²/g – 6.4 cmol₍₊₎/kg, respectively). The wettability values (measurement previously explained in Peyne et al., 2017) also depend on the sampling lot, with higher values for B_y-25 (162–235 and 129–146 $\mu\text{L/g}$ for B_y-25 and A_y-25, respectively). The chemical compositions are consistent and exhibit a significant change, with higher Si/Al and Si/Fe molar ratios for the A_y samples. Fig. 1 shows pictures of the samples before and after the chemical treatment and calcination. The yellow color of the A₁-25 sample is typical for a rich goethite soil (Cornell and Schwertmann, 2002). The calcination at 350 and 700 °C (A₁-350 and A₁-700) leads to a change from yellow to a red color, assigned to the goethite to hematite transformation (Carlos Duarte Cavalcante et al., 2017). The free iron extraction induces a change in color from yellow/orange to gray/white, in agreement with the protocol, which shows that a high amount of goethite content was removed. However, calcination at 350 °C for this sample does not lead to a significant change, with only a slightly darker

¹ Bouyer Leroux, L'établère, 49,280 La Séguinière, France.

Download English Version:

<https://daneshyari.com/en/article/8045931>

Download Persian Version:

<https://daneshyari.com/article/8045931>

[Daneshyari.com](https://daneshyari.com)